2.E *Nuclear Physics* **A183** (1972) 401—416; © *North-Holland Publishing Co., Amsterdam*

OPTICAL-MODEL ANALYSIS OF ^{92,94,96,100}Mo(p, p) FOR 20, 30 AND 50 MeV INCIDENT PROTON ENERGIES

B. C. SINHA, V. R. W. EDWARDS and E. J. BURGE †
Wheatstone Laboratory, King's College, Strand, London WC2, UK
and
W. H. TAIT
Physics Dept., North East London Polytechnic, Romford Rd., Stratford, London E15, UK

Received 20 July 1971
(Revised 8 November 1971)

Abstract: Proton elastic scattering cross sections and polarizations have been measured for several isotopes of molybdenum at 20, 30 and 50 MeV and analysed in terms of the regular optical model, the reformulated optical model and a version of the regular model which contains a real central Saxon-Woods derivative term. New methods are developed for determining the symmetry potential, and the value of employing density-dependent forces in reformulated-model calculations is demonstrated.

E NUCLEAR REACTIONS ^{92,100}Mo(p, p), E = 19.85 MeV; ^{92,94,96,100}Mo(p, p), E = 30.3 MeV; ^{92,96,100}Mo(p, p), E = 49.45 MeV; measured $\sigma(\theta)$; ^{92,96,100}Mo(p, p), E = 30.3 MeV; measured P(θ); deduced optical-model parameters. Enriched targets.

1. Introduction

Recently considerable interest has been shown in the analysis of elastic scattering data with optical potentials derived from nucleonic density functions and the two-body effective interaction [1-7]). Together with this microscopic approach it has been suggested [8-10]) that an additional Saxon-Woods derivative term in the real central part of the optical potential improves the fits and provides an opportunity to investigate the fine structure of the potential from a phenomenological point of view.

We apply these new models in the present paper to our data on proton scattering from isotopes of molybdenum. This data included elastic cross-section measurements for ^{92,100}Mo at 19.85 MeV, for ^{92,94,96,100}Mo at 30.3 MeV and for ^{92,96,100}Mo at 49.45 MeV together with polarization distributions for ^{92,96,100}Mo at 30.3 MeV.

It is particularly interesting to interpret the optical-model parameters for these isotopes in terms of nuclear structure quantities. The $^{92}_{42}Mo_{50}$ nucleus has a closed $1g_{\frac{9}{2}}$ shell for neutrons, and ^{94,96,100}Mo have two, four and eight additional neutrons respectively. The systematic change in the number of excess neutrons from eight in the case of ^{92}Mo to sixteen for ^{100}Mo allows one to investigate the change in the

† Present address: Physics Dept., Chelsea College, University of London, London, UK.

shape of the additional neutron distribution and to study any relationship that may exist between the real depth of the optical potential and the asymmetry parameter $\varepsilon = (N-Z)/A$.

Recently a number of authors [11-14]) have criticized the traditional approach to the determination of the symmetry potential but without advancing a satisfactory alternative. Two possible substitutes are examined in the present paper. The first is to identify the derivative component of the real optical potential in $N > Z$ nuclei with the symmetry term [8]). The theoretical justification for this approach is discussed in sect. 5. The second is a development of the approach of Greenlees *et al.* [5-7]) employing the variation of the volume integral of the real central potential with asymmetry parameter. The poor showing of this method in its original form is probably due to the neglect of second-order terms. The use of a modified formulation based on density-dependent two-body forces which simulate certain second-order effects was shown by Sinha [15]) to improve the method considerably and we have applied this version to our own data in sect. 4.

2. Data collection

The 30.3 and 49.45 MeV data were obtained from experiments on the Proton Linear Accelerator at the Rutherford High Energy Laboratory, and the 19.85 MeV measurements were made at the Variable Energy Cyclotron of the Atomic Energy Research Establishment, Harwell.

The beam from the proton linear accelerator at the Rutherford High Energy Laboratory was momentum analysed using a wedge-shaped bending magnet and two sets of slits to give a FWHM energy spread of $\approx$ 50 keV. It was then focussed onto the target to form a spot 3 mm high by 2 mm wide. The targets used in the cross section measurements were rolled metal foils 5 mg/cm^2 thick mounted on a 1 mg/cm^2 mylar backing at the centre of a 66 cm diam sliding foil scattering chamber [16]). The scattered particles were analysed with an $n = \frac{1}{2}$, 180° magnetic spectrometer. An acoustic spark chamber [17]) mounted in the focal plane of this instrument was used as a position-sensitive detector. The mean energy resolution was $\approx$ 100 keV which was sufficient to separate the elastic peak except at forward angles (10°–28°) where a correction was necessary for the oxygen and carbon in the target backing.

The polarization measurements were made using a polarized ion source which supplied a maximum of $\approx 10^{-4}$ μA on target. The beam polarization B was continuously monitored with a calibrated polarimeter built into the linac and was $\approx$ 50%. The target thickness was increased for these measurements to $\approx$ 40 mg/cm^2 and the overall energy resolution was $\approx$ 150 keV. The polarization P was determined by counting the number of particles scattered with spin up (U) and with spin down (D) using the expression

$$P = \frac{U-D}{U+D} \times \frac{1}{B}. \tag{2.1}$$

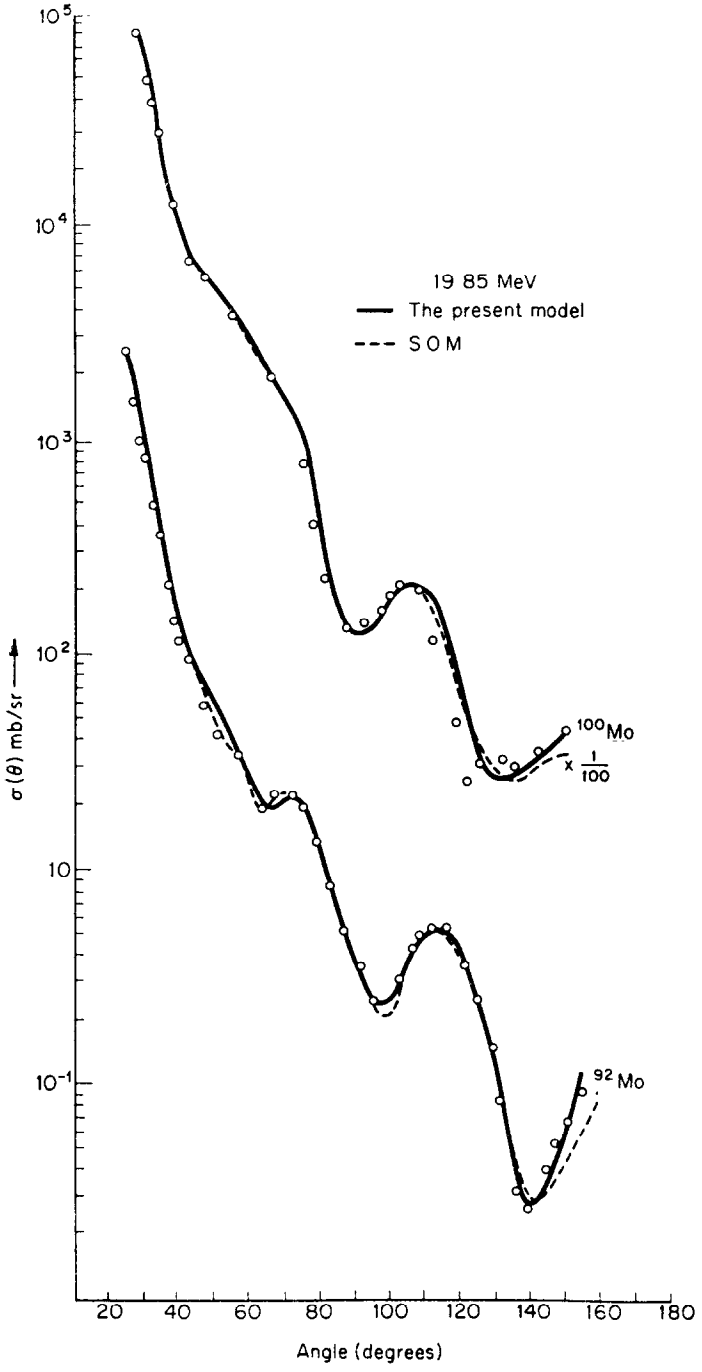

Fig. 1. Comparison of SOM and RDM fits to the ^{92,100}Mo(p, p) cross-section data at $E = 19.85$ MeV.

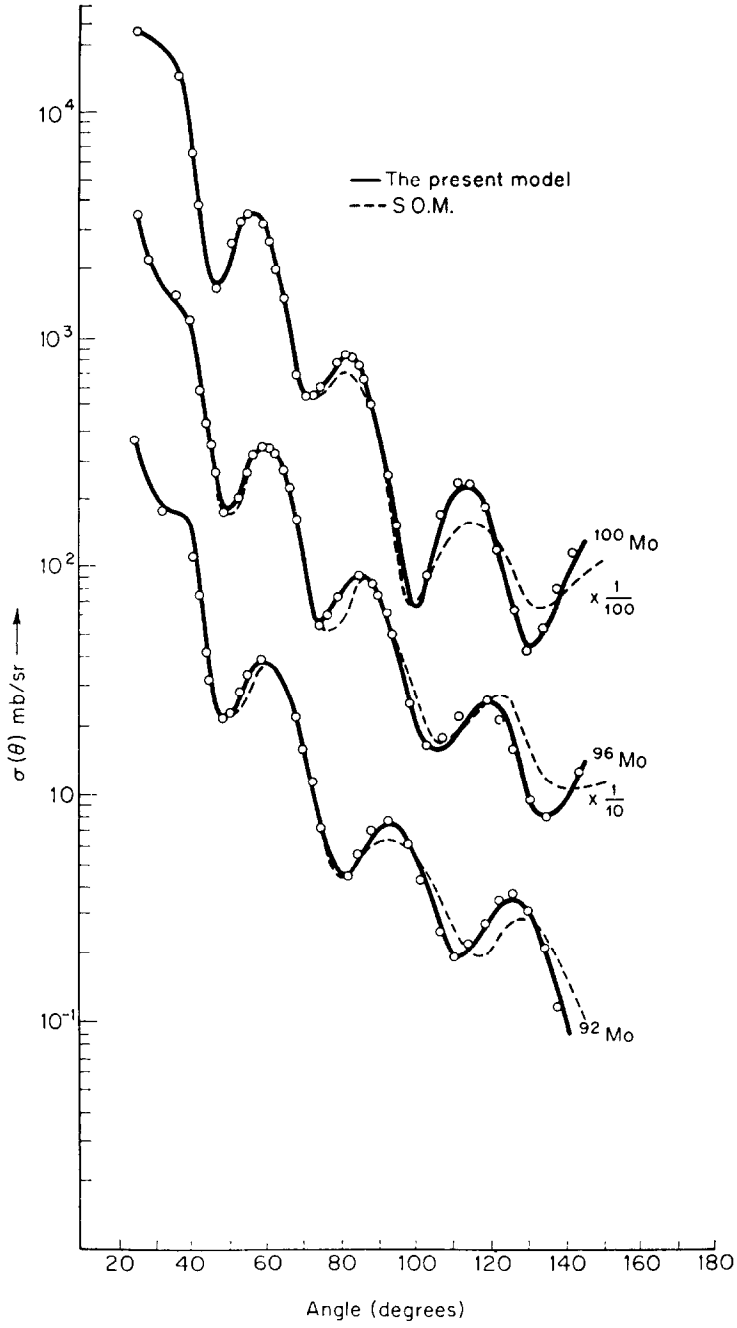

Fig. 2. Comparison of SOM and RDM fits to the ^{92,94,96,100}Mo(p, p) cross section data at $E = 30.3$ MeV.

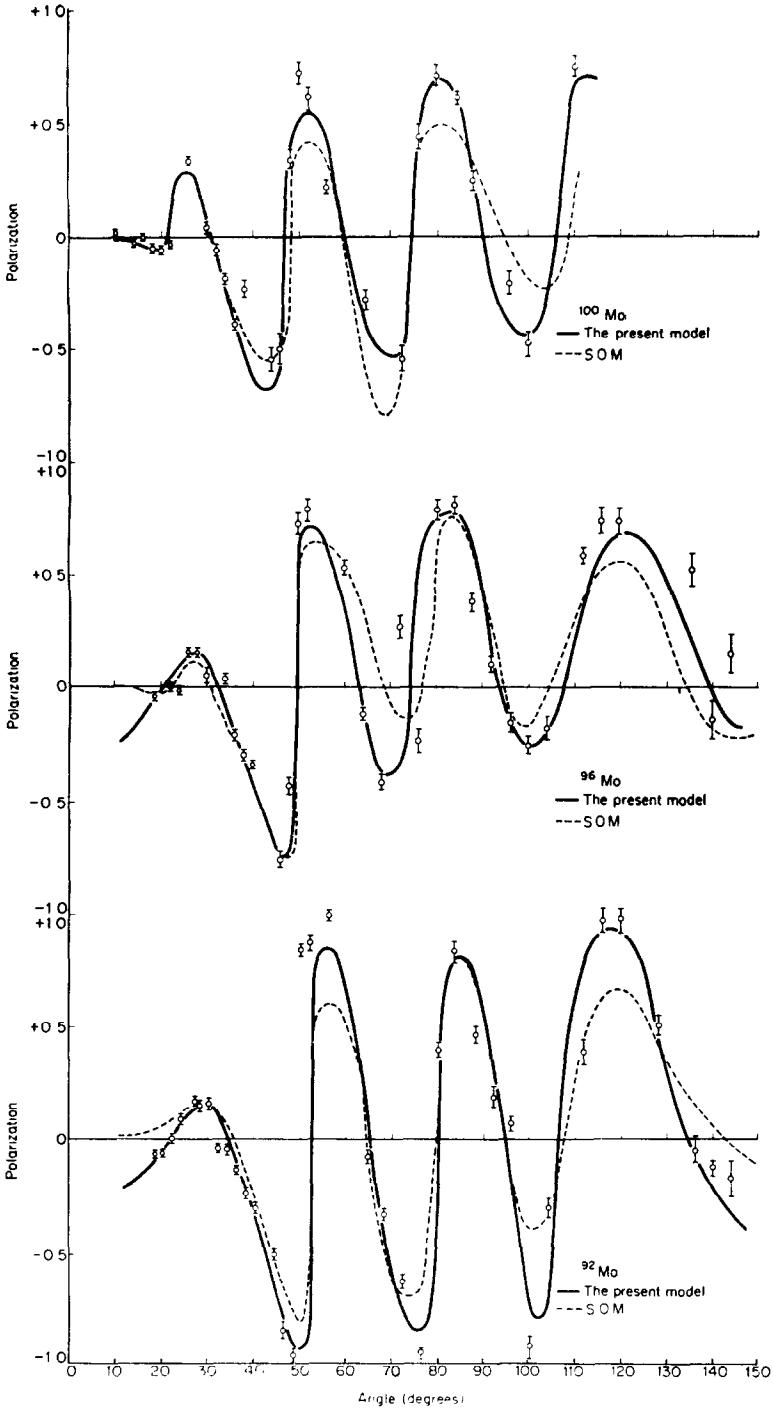

Fig. 3. Comparison of SOM and RDM fits to the ^{92,96,100}Mo(p, p) polarization data at $E = 30.3$ MeV.

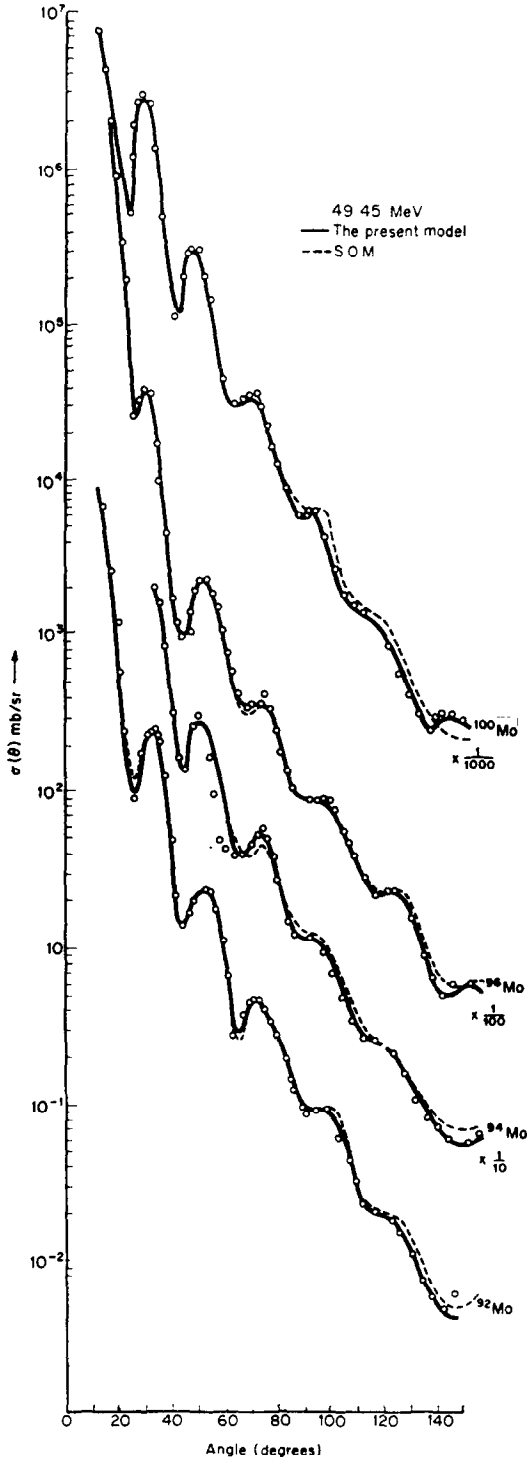

Fig. 4. Comparison of SOM and RDM fits to the ^{92,96,100}Mo(p, p) cross section data at $E = 49.45$ MeV.

The measurements on the variable energy cyclotron were made with a counter telescope consisting of a 4 mm thick lithium-drifted silicon E-detector and a 400 μm diffused surface-barrier ΔE counter. Since the Q-values for reaction processes induced by incident protons are negative it was not necessary to employ particle discrimination circuitry.

The cross section and polarization results are plotted in figs. 1–4. The cross section errors are too small to show on the graphs. They are fairly constant through the angular range and are typically $\approx 4\,\%$, most of which is statistical and the remainder is due mainly to a 1 % uncertainty in target thickness. The errors shown for the polarization are largely statistical and varied between ± 0.03 at forward angles and ± 0.1 at backward angles.

All the data are uncorrected for the finite angular spread of the scattered protons, which was $\approx 0.6°$ for the cross sections and $\approx 1°$ for the polarizations. Corrections for this angular resolution were made in the theoretical fits but did not perceptibly alter the results of the analyses.

3. Simple optical-model analysis (SOM)

For this analysis the optical potential was taken to have the form

$$U_{\mathrm{OPT}}(r) = U_{\mathrm{C}}(r) - U_{\mathrm{R}} f(x_{\mathrm{R}}) - i\left(W_{\mathrm{V}} - 4W_{\mathrm{D}} \frac{\mathrm{d}}{\mathrm{d}x_{\mathrm{I}}}\right) f(x_{\mathrm{I}}) + \left(\frac{\hbar}{m_\pi c}\right)^2 V_{\mathrm{s.o.}} \frac{1}{r}\left(\frac{\mathrm{d}f(x_{\mathrm{s.o.}})}{\mathrm{d}r}\right) \boldsymbol{\sigma} \cdot \boldsymbol{l}, \quad (3.1)$$

where $U_{\mathrm{C}}(r)$ is the Coulomb potential for a uniformly charged sphere of radius $1.25\, A^{\frac{1}{3}}$ fm and

$$\begin{aligned} f(x) &= (\mathrm{e}^x + 1)^{-1}, \\ x_{\mathrm{R}} &= (r - r_{\mathrm{R}} A^{\frac{1}{3}})/a_{\mathrm{R}}, \\ x_{\mathrm{I}} &= (r - r_{\mathrm{I}} A^{\frac{1}{3}})/a_{\mathrm{I}}, \\ x_{\mathrm{s.o.}} &= (r - r_{\mathrm{s.o.}} A^{\frac{1}{3}})/a_{\mathrm{s.o.}}. \end{aligned} \quad (3.2)$$

The calculations were performed with the computer code RAROMP 1 written by Pyle. This included a search program which minimized the quantity

$$\chi_{\mathrm{T}}^2 = \chi_\sigma^2 + \chi_{\mathrm{P}}^2,$$

where

$$\begin{aligned} \chi_\sigma^2 &= \sum_i^{N_\sigma} \left\{\frac{\sigma_{\mathrm{th}}(\theta_i) - \sigma_{\mathrm{exp}}(\theta_i)}{\delta\sigma(\theta_i)}\right\}^2, \\ \chi_{\mathrm{P}}^2 &= \sum_i^{N_{\mathrm{P}}} \left\{\frac{P_{\mathrm{th}}(\theta_i) - P_{\mathrm{exp}}(\theta_i)}{\delta P(\theta_i)}\right\}^2, \end{aligned} \quad (3.3)$$

N_σ and N_P are the number of cross sections and polarization data points, $\sigma_{th}(\theta_i)$ and $\sigma_{exp}(\theta_i)$ are respectively the theoretical and experimental cross sections at the angle θ_i, $\delta\sigma(\theta_i)$ is the uncertainty in the cross section and $P_{th}(\theta_i)$, $P_{exp}(\theta_i)$ and $\delta P(\theta_i)$ are similar quantities for the polarization.

The data analysed consisted of our own 30.3 MeV polarizations and 19.85, 30.3 and 49.5 MeV cross sections together with the 20.25 MeV ^{92}Mo polarization measurements of Glashausser *et al.* [18]). The difference of about 0.4 MeV between the incident energies employed for our cross-section measurements and the polarization measurements of Glashausser *et al.* is greater than is desirable and may have slightly affected the 20 MeV ^{92}Mo analysis. Starting from the average geometry of Fricke *et al.* [19]) the parameters of the model were varied systematically until convergence was achieved. The results are compared with those found using the additional Saxon-Woods derivative term in table 1. Somewhat low values were obtained for r_R at 20 MeV. These appear to be genuine and not the result of obtaining a false minimum.

TABLE 1

Optical-model parameters obtained in the SOM and RDM analyses

SOM	RDM	^{92}Mo			^{94}Mo	^{96}Mo		^{100}Mo		
energy (MeV)		19.85	30.3	49.4	49.4	30.3	49.4	19.85	30.3	49.4
U_R		59.15	51.76	49.77	48.09	53.69	49.99	57.25	51.40	52.89
	U_R	55.72	52.30	42.29	42.93	44.72	38.50	50.15	41.03	36.56
r_R		1.121	1.161	1.153	1.140	1.156	1.150	1.132	1.172	1.140
	r_R	1.125	1.165	1.124	1.132	1.178	1.146	1.245	1.238	1.182
a_R		0.780	0.773	0.754	0.870	0.795	0.740	0.740	0.878	0.830
	a_R	0.750	0.792	0.740	0.750	0.756	0.750	0.742	0.770	0.780
	U_S	4.25	3.05	2.10	2.50	4.25	3.29	6.51	5.92	4.95
	r_S	0.887	0.892	0.920	0.941	0.897	0.962	0.985	0.957	1.050
	a_S	0.760	0.770	0.760	0.750	0.751	0.760	0.740	0.750	0.750
W_V		1.75	3.14	9.69	10.76	5.74	8.77	1.35	4.89	5.81
	W_V	1.25	2.15	8.45	8.92	4.95	6.52	1.24	3.25	4.92
W_D		9.45	4.35	1.53	0.46	2.59	1.97	8.68	6.40	5.13
	W_D	10.25	5.21	1.85	1.02	3.62	2.50	9.52	5.94	6.25
r_I		1.298	1.357	1.310	1.350	1.420	1.300	1.370	1.354	1.200
	r_I	1.320	1.372	1.352	1.362	1.392	1.351	1.375	1.372	1.360
a_I		0.612	0.616	0.629	0.632	0.589	0.660	0.672	0.573	1.150
	a_I	0.652	0.642	0.630	0.640	0.621	0.630	0.592	0.684	0.630
$V_{s.o.}$		5.49	6.46	6.02	7.66	7.36	7.09	6.27	8.61	7.42
	$V_{s.o.}$	5.62	5.95	6.24	7.59	6.92	6.39	6.52	7.52	7.52
$r_{s.o.}$		1.055	1.004	1.100	0.938	1.018	1.047	1.106	1.051	1.002
	$r_{s.o.}$	1.059	1.052	1.062	1.059	1.035	1.042	1.082	1.062	1.002
$a_{s.o.}$		0.678	0.594	0.784	0.550	0.660	0.748	0.652	0.559	0.870
	$a_{s.o.}$	0.721	0.672	0.750	0.750	0.690	0.750	0.674	0.623	0.790
χ_σ^2/N_σ		11.95	7.53	10.70	12.50	10.24	9.00	10.25	11.53	9.50
	χ_σ^2/N_σ	4.25	4.25	4.95	4.22	6.52	6.50	4.95	7.25	3.15
χ_P^2/N_P		7.52	11.20			11.25			14.52	
	χ_P^2/N_P	3.15	6.28			5.62			5.45	

Rather different parameters and lower χ^2 values were obtained by Glashausser *et al.* probably because their cross-section data had a different distribution of errors to our own. As can be seen from figs. 1–4, the fits to the scattering data are quite satisfactory in general, although they deteriorate at backward angles, especially for ^{100}Mo.

4. Reformulated optical-model analysis (ROM)

This part of the analysis was based on the model proposed by Greenlees, Pyle and Tang [7]) and was completed using a computer program supplied by Pyle.

In the reformulated model the Coulomb and imaginary parts of the optical potential are the same as for the regular model, but the real central and spin-orbital potentials are obtained from the nuclear matter distribution and the nucleon-nucleon force assuming that the direct and isospin-dependent parts U_D and U_τ of the two-nucleon potential have the same form factors so that

$$U_\tau(r) = -\zeta U_D(r), \tag{4.1}$$

where ζ is a constant and r is the separation of the interacting nucleons.

The real central potential $V_R(r)$ is given by

$$V_R(r) = -V_R I(r)/I(0), \tag{4.2}$$

where the adjustable coefficient V_R is used to take care empirically of any omissions in the formulation and $I(r)$ is expressed in terms of the matter distribution ρ_m and the nucleon-nucleon force:

$$I_m(r) = \int \rho_m(r') U_D(|r-r'|) \mathrm{d}r', \tag{4.3}$$

where $\rho_m(r)$ is assumed to have a Saxon-Woods form and the radius and diffuseness parameters r_m and a_m of this distribution are treated as variable parameters.

The spin-orbit potential is also related to the microscopic nuclear properties by a similar expression:

$$V_S(r) = -\int \rho_m(r') U_{ls}(|r-r'|) \left[\frac{r \cdot r'}{r^2} - 1\right] \mathrm{d}r', \tag{4.4}$$

where U_{ls} is the two-nucleon spin-orbital interaction. This expression can be used in full, as in the present work, or in an approximate first-order form which corresponds to the usual Thomas term of the regular model.

In Pyle's program U_D and U_{ls} are assumed to have Yukawa form factors and their ranges may be set by reading in the corresponding mean square radii $\langle r^2 \rangle_D$ and $\langle r^2 \rangle_{ls}$. The latter was set equal to 0.5 fm^2 as recommended in ref. [6]). The value of $\langle r^2 \rangle_D$ was chosen to give an optimum fit to the 30 MeV ^{96}Mo data using the automatic gridding facility in the program. A value of 2.25 fm^2 was obtained and employed for all the

analyses described below. Similar values were found by Greenlees *et al.* in their earlier work [7]) and by other authors employing Yukawa forces. Most recent ROM calculations have however used Gaussian forces and require $\langle r^2\rangle_D \approx 4$ fm^2. Low-energy nucleon-nucleon scattering data has been fitted with Gaussian forces having an average $\langle r^2\rangle_D \approx 4.3$ fm^2 and with Yukawa forces with $\langle r^2\rangle_D$ in the range 1.5–3.5 fm^2. The OPEP model predicts a Yukawa form factor with $\langle r^2\rangle_D \approx 3$ fm^2.

The fits to the elastic scattering data provided by the ROM were very similar to those produced by the SOM and for this reason we have not shown them in figs. 1–4. The parameters obtained are listed in table 2. We used these values to calculate ζ and the difference between the neutron and proton mean square radii $\Delta = \langle r^2\rangle_n - \langle r^2\rangle_p$.

The latter quantity was found using the relation

$$A\langle r^2\rangle_m = N\langle r^2\rangle_n + Z\langle r^2\rangle_p, \tag{4.5}$$

TABLE 2

Optical-model parameters obtained in the ROM analyses

Energy (MeV)	^{92}Mo			^{94}Mo	^{96}Mo		^{100}Mo		
	19.85	30.3	49.45	49.45	30.3	49.45	19.85	30.3	49.45
U_R	58.56	55.89	53.69	51.58	53.52	49.28	55.98	53.28	58.28
r_m	1.139	1.121	1.137	1.162	1.154	1.158	1.157	1.179	1.087
a_m	0.620	0.657	0.681	0.721	0.794	0.695	0.792	0.675	0.760
W_V	0.62	2.53	13.08	9.26	4.36	10.22	1.63	2.69	12.69
W_D	9.25	5.95	0.36	2.54	4.62	1.29	10.92	9.58	1.00
r_I	1.356	1.356	1.350	1.350	1.350	1.350	1.350	1.328	1.350
a_I	0.670	0.628	0.630	0.630	0.630	0.630	0.630	0.615	0.630
$V_{s.o.}$	1989	1922	1966	2251	2079	2158	2076	2075	2285
χ_σ^2/N_σ	12.80	9.42	6.81	9.50	9.58	10.20	14.78	16.52	12.50
χ_P^2/N_P		10.95			11.68			9.25	
$\langle r^2\rangle_m$	20.72	21.05	20.85	21.75	23.85	25.52	25.98	24.92	24.95

TABLE 3

Results for ζ and Δ

Isotope	Energy (MeV)	$\zeta = AJ_S/(N-Z)J_R$	Δ^{ROM} (fm^2)	Δ^{RDM} (fm^2)
^{92}Mo	19.85	0.54±0.02	5.02	0.72±0.30
^{100}Mo	19.85	0.71±0.02	10.52	2.76±0.30
^{92}Mo	30.3	0.50±0.02	7.05	0.80±0.30
^{96}Mo	30.3	0.48±0.02	9.65	0.97±0.30
^{100}Mo	30.3	0.69±0.02	9.72	2.93±0.30
^{92}Mo	49.5	0.53±0.02	7.63	0.75±0.30
^{94}Mo	49.5	0.59±0.02	8.50	1.21±0.30
^{96}Mo	49.5	0.48±0.02	7.95	1.25±0.30
^{100}Mo	49.5	0.70±0.02	8.90	3.10±0.30

and assuming that the proton distribution had a Saxon-Woods form with the radius and diffuseness parameters given by the formula of Acker *et al.* [20]) as modified by Greenlees *et al.* [7]):

$$r_p = (1.106 + 1.05 \times 10^{-4} A)\ \text{fm}, \qquad (4.6)$$
$$a_p = 0.454\ \text{fm}.$$

The results for Δ shown in the fourth column of table 3 vary between 6 and 10 fm^2 and tend to increase as A increases, indicating that the additional neutrons may be distributed at a larger radius than the protons.

However these values of Δ are somewhat larger than those found by other authors [refs. [21-23])]. It is well known that the figures obtained for Δ by this method are very sensitive to the value chosen for $\langle r^2 \rangle_D$, and since the latter is not well determined by the ROM the disagreement is not surprising. As we shall show in sect. 5 it is possible to extract values for Δ which are independent of $\langle r^2 \rangle_D$ from the derivative component of the real optical potential.

Recently Greenlees *et al.* [14]) pointed out that the linear dependence of U_R on $\varepsilon = (N-Z)/A$ often found in proton elastic scattering analyses is fortuitous and is due to the choice of constant values for r_R and a_R. They propose an alternative method of studying the symmetry effects based on the variation of the volume integral J_{RS} of the real potential

$$J_{RS}/A = J_D + \varepsilon J_\tau, \qquad (4.7)$$

where J_D and J_τ are the volume integrals of the Wigner and isospin-dependent components of the two-body force. Their ratio is equal to $-\zeta$ if identical form factors are assumed for the two components. This method has been found to give inconsistent and low values for the symmetry term, probably because of the approximations made in deriving the ROM and eq. (4.7) which is based on it.

The most important of these approximations is possibly the neglect of second- and higher-order terms arising predominantly from the tensor force. The effects of the tensor force can be conveniently simulated by a density-dependent interaction as suggested by Bethe [24]). Friedman [25]) has shown that using the strong density-dependent effective interaction of Green [26]) explains the discrepancy between the results of the ROM and the Coulomb displacement energies [23]). Following Friedman's work, one of the authors (B.C.S.) [15]) derived an expression for the volume integral of the real potential using a linear density-dependent force proposed by Lande *et al.* [27]):

$$(J_{RS}/A)_C = J_D(1 + \alpha_D S_m) + \varepsilon J_\tau (1 + \alpha_\tau S_m). \qquad (4.8)$$

Here, $a_D = 0.67$ and $\alpha_\tau = 1.61$ are the parameters in the strong density-dependent force and S_m is defined by

$$S_m = \frac{3a_m}{R_m}\left(1 - \frac{2\pi^2 a_m^2}{3R_m^2}\right),$$
$$R_m = r_m A^{\frac{1}{3}}. \qquad (4.9)$$

The subscript C has been appended to $(J_{RS}/A)_C$ to indicate that it has been corrected for non-local Coulomb effects by the method described in ref. [15]). Because S_m is itself a function of A, it is clear from eq. (4.8) that it is not possible to obtain a simple linear relation between J_{RS}/A and J_τ of the form of eq. (4.7).

In the upper part of fig. 5 $(J_{RS}/A)_C(1+\alpha_D S_m)^{-1}$ has been plotted as a function of $\varepsilon(1+\alpha_\tau S_m)(1+\alpha_D S_m)^{-1}$ for a range of elements at 30 and 50 MeV. This graph should

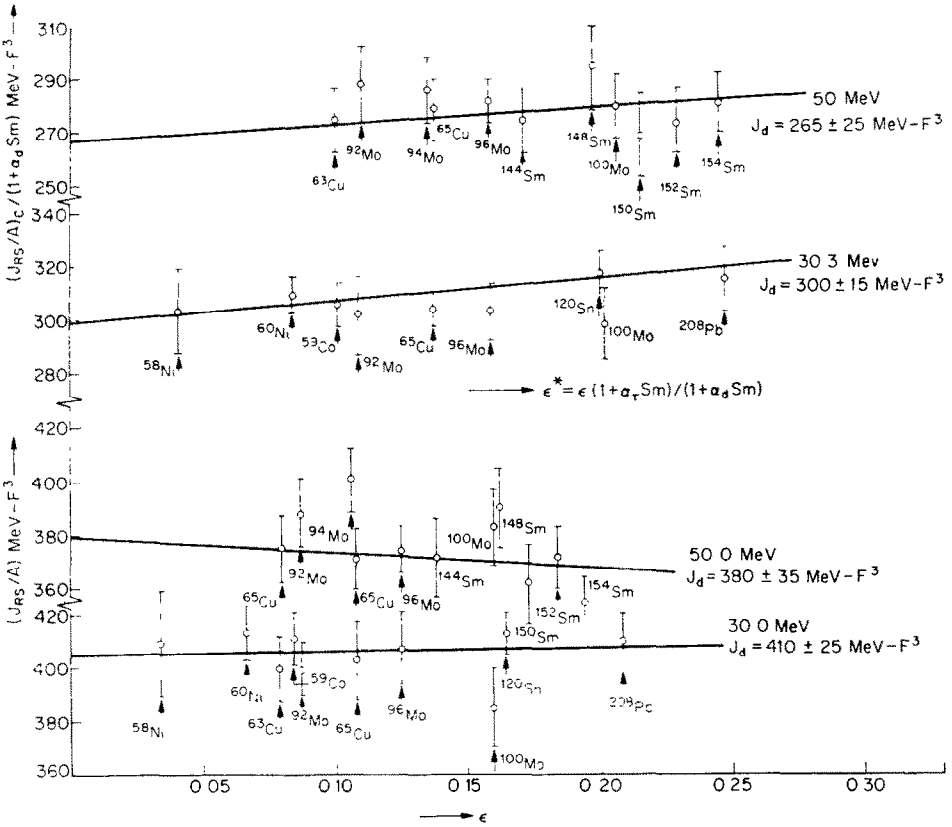

Fig. 5. Systematics of the volume integral of the real central potential with density-dependent and density-independent forces.

be compared with the lower part of the same figure which shows the variation of J_{RS}/A as a function of ε. At 50 MeV the samarium data are taken from ref. [28]) and the copper data from ref. [29]). The 30 MeV points other than the molybdenum ones are from ref. [6]). It is evident that with the density-dependent force an improved linear dependence is obtained and, furthermore, the gradient, which is equal to J_τ, shows a definite consistency between the two energies in contrast to the conclusions of Greenlees *et al.* [6]). The value of $\zeta = -J_D/J_\tau$, obtained with the density dependent force, subject to considerable error, lies in the range 0.3–0.7. The magnitude of J_D shows the

same trend with energy as found in ref. [7]), although smaller by ≈ 130 MeV · fm^3, the decrease being characteristic of this type of effective interaction [30]). In order to facilitate the comparison with earlier analyses we have not corrected the lower part of fig. 5 for non-local Coulomb effects. Had this been done, the slopes of the J_{RS}/A versus ε-lines and hence the corresponding values of ζ would have been negative.

5. The real derivative model analysis (RDM)

The model was developed from the SOM by adding a real central Saxon-Woods derivative term of the form

$$4U_S a_S \frac{d}{dr} f(r, r_S, a_S). \tag{5.1}$$

As can be seen from figs. 1–4 the RDM gives consistently better fits to the data than the SOM, the improvement being most marked at backward angles and for ^{100}Mo. Typically χ^2 is reduced by a factor of 2–3. However, because of its dependence on the errors used for weighting the data points, the reduction in χ^2 is not an unambiguous measure of the improvement in fit. As judged by eye the improvement is most striking at 30 MeV, less noticeable at 50 MeV and almost undetectable at 20 MeV. Yet the reduction in χ^2 is smallest at 30 MeV.

Table 1 lists the parameters obtained with this model. The depth of the derivative term, U_S, increases steadily from ^{92}Mo to ^{100}Mo at a particular energy and decreases as the incident proton energy is raised. The radius of the derivative term, r_S, remains more or less constant for a given isotope at all energies, although it increases with neutron number.

As mentioned in ref. [10]) a number of effects may be responsible for the derivative term and little is known about their relative magnitudes. Of the most likely causes, namely exchange, target polarization, the hard core of the effective nucleon-nucleon interaction and symmetry effects arising from the excess neutrons, only the latter is easily calculable. We have therefore concentrated on this effect in our efforts to relate the derivative term to something more fundamental. At first this seemed an unpromising line because both our own fits [10]) and those of Boyd *et al.* [9]) had shown that there was an appreciable derivative term even in $N = Z$ nuclei. Moreover the symmetry potentials generated by folding the excess neutron distribution of the shell model with an effective two-body isospin-dependent force appear to have a pure Saxon-Woods derivative shape only for nuclei with a small neutron excess [31]). Despite this discouraging situation we examined the consequences of assuming that the symmetry potential and the derivative term could be completely identified with each other for $N > Z$ nuclei. This extremely simple model has given a very successful account of the results obtained from such nuclei. The first indication of its promise was supplied by our earlier work on ^{208}Pb in ref. [8]) where the double magic structure and the availability of (p, n) cross section and Coulomb displacement energy data permitted a close

test to be made of the hypothesis. Unfortunately such a detailed examination is not possible for the Mo isotopes. However, the systematic increase of the depth and the radius of the derivative term from ^{92}Mo to ^{100}Mo is in agreement with the interpretation of the derivative potential as arising from symmetry effects. Later in this section we calculate the values of Δ and ζ on the basis of this model and obtain an impressive consistency among the large number of results.

The surprising practical success of our model must in part be fortuitous, but it may also reflect the existence of previously unsuspected effects. Two possibilities come to mind. The first is an unexpected rapid decrease of hard core, target polarization, exchange and density-dependent contributions with increasing A-number, possibly due to accidental cancellation of effects with contrary tendencies. Thus although these effects may be important for the derivative terms of the relatively light $N = Z$ nuclei they may be negligible in heavier targets. The second is that there may be a tendency for exchange and target polarization effects to make their contributions predominantly through the symmetry potential in $N > Z$ nuclei. Thus identifying the derivative and the symmetry potentials implicitly takes these other contributions into account to a great extent. Owen and Satchler [2]) showed that exchange effects enhance the symmetry potential by $\approx 30\,\%$. In addition, for heavy non-collective nuclei the quasi-elastic (p, n) cross section is often greater than the cross section for inelastic scattering to the lowest excited states. Despite the high excitation energy involved, it may therefore be possible that the dominant intermediate states involved in second-order effects with such nuclei are in the charge-exchange channels. This would give rise to target polarization effects which are strongly dependent on the τ_z of the incident particle.

In order to test our model on the Mo results we have calculated Δ and ζ assuming the derivative term to be entirely produced by the symmetry potential. These quantities were obtained from expressions derived in ref. [8]):

$$\Delta = \frac{N^2-Z^2}{2NZ}\{\langle r^2\rangle_S - \langle r^2\rangle_R\}, \tag{5.2}$$

$$\zeta = \frac{AJ_S}{(N-Z)J_R}, \tag{5.3}$$

where $\langle r^2\rangle_S$ and $\langle r^2\rangle_R$ are the mean square radii of the real derivative and real Saxon-Woods potentials respectively and J_S and J_R are the corresponding volume integrals.

The results obtained for ζ are presented in the third column of table 3. In all cases except ^{100}Mo it is close to the accepted value of ≈ 0.48, which to a great extent supports our identification of the derivative term with the symmetry potential.

The values obtained for Δ are listed in the fifth column of table 3. It will be seen that consistent values are produced for a given isotope at all the energies employed and that there is a smooth increase of Δ from ≈ 0.7 in the case of ^{92}Mo to ≈ 3.1 fm^2 for ^{100}Mo. In agreement with recent nuclear structure calculations [21, 22]) and the work of Zimanyi *et al.* [31]) with the Lane equations, much smaller values of Δ are

obtained by the present method than by the ROM. The chief merit of this new method is that the results do not depend on $\langle r^2 \rangle_D$. However considerable uncertainties are introduced by possible contributions to the derivative term made by effects other than the symmetry potential.

RDM analyses similar to the above have been made for a large number of nuclei at several energies and the results are summarized in ref. [10]). Our overall conclusion both from that work and the present is that a real derivative term is definitely required in the optical potential and that it will substantially improve the fit to most elastic scattering data. This conclusion is supported by the work of Boyd *et al.* [9]) on ^{16}O and ^{40}Ca but is opposed by that of Perey [32]). He has criticized our first paper on the RDM [8]) on the grounds that only cross-section data was fitted. He reanalysed the ^{208}Pb scattering data, representing the real potential form factor by a combination of a Gaussian term centered at the origin and a modified Saxon-Woods function with different diffuseness parameters inside and outside the halfway radius. Although fits to cross-section data alone were considerably improved by the new degrees of freedom permitted to the real form factor, there was very little change in the quality of fits made simultaneously to cross-section and polarization data. He concluded that the results we had obtained for ^{208}Pb in ref. [8]) were misleading. This work was our earliest on the RDM and subsequent analyses on other targets have involved simultaneous fits to cross-section and polarization data when the latter was available. These analyses have all confirmed our original conclusions both as to the improvement in χ^2 and as to the parameters of the derivative potential. Moreover we have observed little difference in the present work between cases which included polarization data and those for which it had not been measured. In the light of these facts, we suggest that Perey's disquieting results show either that this method of parametrizing the real form factor is unsatisfactory or else that he has not found the best minimum in χ^2 space, which is often a difficult task when there are so many parameters.

6. Conclusions

The work presented here shows that an additional Saxon-Woods derivative term in the real optical potential gives a worthwhile improvement in the fits to elastic scattering data. It also demonstrates the usefulness of two new methods of determining the symmetry potential and indicates that a density-dependent nucleon-nucleon interaction is more appropriate for ROM calculations than the usual Gaussian force.

We acknowledge with gratitude the encouragement and assistance received from R. J. Griffiths, G. Squires, C. J. Marchese, P. B. Wollam, G. L. Thomas, N. M. Clarke and other members of the King's College group and the staff of the Rutherford High Energy and the Harwell Variable Energy Cyclotron Laboratories.

References

1) G. L. Thomas and B. C. Sinha, Phys. Rev. Lett. **26** (1971) 325
2) L. W. Owen and G. R. Satchler, Phys. Rev. Lett. **25** (1970) 1720
3) D. Slanina and H. McManus, Nucl. Phys. **A116** (1968) 271
4) K. H. Kidawi, Ph.D. thesis, 1969, Oxford University, unpublished
5) G. W. Greenlees, V. Hnizdo, O. Karban, J. Lowe and W. Makofske, Phys. Rev. **2C** (1970) 1063
6) G. W. Greenlees, W. Makofske and G. J. Pyle, Phys. Rev. **1C** (1970) 1145
7) G. W. Greenlees, G. J. Pyle and Y. C. Tang, Phys. Rev. **171** (1968) 1115
8) B. C. Sinha and V. R. W. Edwards, Phys. Lett. **31B** (1970) 273
9) R. N. Boyd, J. C. Lombardi and R. Mohan, preprint, Rutgers University
10) B. C. Sinha and V. R. W. Edwards, Phys. Lett. **35B** (1971) 391
11) G. L. Thomas, Communications of Montreal Conf. on properties of nuclear states (Les Presses de l'Université de Montréal 1969) p. 255
12) P. E. Hodgson, Nucl. Phys. **A150** (1970) 1
13) C. M. Perey and F. G. Perey, Phys. Lett. **26B** (1968) 123
14) G. W. Greenlees, G. J. Pyle and Y. C. Tang, Phys. Lett. **26B** (1968) 658
15) B. C. Sinha, Phys. Lett. **33B** (1970) 280
16) J. A. Fannon, E. J. Burge, D. A. Smith and N. K. Ganguly, Nucl. Phys. **A97** (1967) 263
17) A. G. Hardacre, Nucl. Instr. **52** (1967) 309
18) C. Glashausser *et al.*, Phys. Rev. **184** (1969) 1217
19) M. P. Fricke *et al.*, Phys. Rev. **156** (1967) 1207
20) H. A. Acker *et al.*, Nucl. Phys. **87** (1966) 1
21) J. W. Negele, Phys. Rev. **1C** (1970) 1260
22) V. R. Pandharipande, Phys. Lett. **29B** (1969) 1
23) J. A. Nolen, J. P. Schiffer and N. Williams, Phys. Lett. **27B** (1968) 1
24) H. Bethe, Proc. Tokyo Conf. on nuclear structure phyics **4** (1970) 75
25) E. Friedman, Phys. Lett. **29B** (1969) 213
26) A. M. Green, Phys. Lett. **24B** (1967) 384
27) A. Lande, A. Molinari and G. E. Brown, Nucl. Phys. **A115** (1968) 241
28) P. B. Wollam *et al.*, Nucl. Phys. **A179** (1972) 657
29) G. L. Thomas, E. J. Burge and D. A. Smith, Nucl. Phys. **A171** (1971) 165
30) G. E. Brown, Comments on Nucl. and Part. Phys. **4** (1970) 75
31) J. Zimanyi and B. Gyrmali, Phys. Rev. **174** (1968) 1112
32) F. G. Perey, Polarization phenomena in nuclear reactions, 1971 (University of Wisconsin Press) p. 131